

Thermal Characterization Testing of a Robust and Reliable Thermal Knife HDRM (Hold Down and Release Mechanism) for CubeSat Deployables

Joseph Thompson^{1,4}, David Murphy^{2,4}, Jack Reilly^{2,4}, Lána Salmon^{2,4}, Rachel Dunwoody^{2,4}, Maeve Doyle^{2,4}, Sarah Walsh^{2,4}, Sai Krishna Reddy Akarapu^{2,4}, Jessica Erka^{2,4}, Gabriel Finneran^{2,4}, Joseph Mangan^{2,4}, Fergal Marshall^{3,4}, Loris Franchi⁵, Lily Ha⁶, David Palma⁵, Alexey Ulyanov^{2,4}, Antonio Martin-Carrillo^{2,4}, Sheila McBreen^{2,4}, William O'Connor^{1,4}, Ronan Wal^{2,4}, Lorraine Hanlon^{2,4} and David McKeown^{1,4}

Abstract

Thermal knife HDRMs (Hold Down and Release Mechanisms) are commonly used in CubeSats and other small satellites. However, detailed information on proven designs is difficult to find. Design of a robust and reliable mechanism can present technical challenges which may only become apparent during testing, and often only when tested in a space representative environment.

A custom thermal knife HDRM was designed and built for the antenna deployment module of EIRSAT-1 to deploy four coil spring antenna elements, but the same or a similar design could be repurposed quite easily to release a wide range of CubeSat deployables. In this design resistors are used to cut dyneema lines.

For robustness and reliability, the thermal response of the mechanism must be well understood. To reach the melting point of the dyneema (150C) the power dissipated in the resistors must often exceed the maximum rated value. Therefore, choosing the operating current and the burn time is a careful trade-off between ensuring that the resistor reliably cuts the dyneema line and ensuring that the resistor, solder joints, PCB and nearby components are not damaged by the high temperatures. These choices are further complicated by the requirement that the mechanism operates over a range of temperatures.

A thermal vacuum test campaign was carried out to better understand and characterise the thermal behaviour of the EIRSAT-1 mechanism. For the test a model of the mechanism was built with several temperature sensors installed. Two of these sensors were installed directly on the body of the resistors using a thermally conductive epoxy. Burn tests were performed in vacuum at temperatures between -37C and +56C.

The test shows many interesting results including the effect of the dyneema lines on the thermal response, the possibility of desoldering the burn resistors and a comparison between the performance at ambient and vacuum conditions. Finally, a summary is given of the key technical challenges associated with this type of mechanism along with some recommendations to help make future designs more robust and reliable.

Keywords

CubeSat Deployable, EIRSAT-1, Hold Down and Release Mechanism, Thermal Knife

¹ School of Mechanical and Materials Engineering, University College Dublin, Belfield, Dublin 4, Ireland

² School of Physics, University College Dublin, Belfield, Dublin 4, Ireland

³ School of Computer Science, University College Dublin, Belfield, Dublin 4, Ireland

⁴ Centre for Space Research, University College Dublin, Belfield, Dublin 4, Ireland

⁵ Redu Space Services for European Space Agency, ESEC, Belgium

⁶ HE Space Operations for European Space Agency, ESTEC, The Netherlands

Acronyms/Abbreviations

<i>ADM</i>	<i>Antenna Deployment Module</i>
<i>EGSE</i>	<i>Electrical Ground Support Equipment</i>
<i>EIRSAT</i>	<i>Educational Irish Research Satellite</i>
<i>HDRM</i>	<i>Hold Down and Release Mechanism</i>
<i>UCD</i>	<i>University College Dublin</i>
<i>UHMWPE</i>	<i>Ultra-High Molecular Weight Polyethylene</i>

1. Introduction

Thermal knife HDRMs (Hold Down and Release Mechanisms) are commonly used in CubeSats and other small satellites to constrain deployables before release on orbit [1, 2]. These mechanisms typically use a tensioned meltline (usually a short piece of fishing line) to hold a spring-actuated deployable element in place. The meltline passes over a heating element which thermally cuts the line when activated, releasing the deployable element. These mechanisms are present in many commercial CubeSat products and therefore have extensive flight heritage. However, detailed information on proven designs is difficult to find in the literature. Design of a robust and reliable thermal knife mechanism using inexpensive components, as may be required in university CubeSat projects, can present technical challenges which may only become apparent during testing, and often only when they are tested in a space representative environment [3], which may not be feasible early in the project.

EIRSAT-1 (Educational Irish Research Satellite 1) [4] is a 2U CubeSat being built by students and staff at UCD (University College Dublin) as part of ESA Education's "Fly Your Satellite! 2" programme. A custom thermal knife HDRM was designed and built at UCD for this mission. On EIRSAT-1, the HDRM is used in the ADM (Antenna Deployment Module) [5] to deploy four coil spring antenna elements, but the same or a similar design could be repurposed quite easily to release a wide range of CubeSat deployables, including solar panels, large antennas, drag sails and booms. In the ADM mechanism the meltline material is UHMWPE (Ultra High Molecular Weight Polyethylene). Also known as dyneema, this material was chosen mainly for its relatively low melting point of approximately 150C. In this case the heating elements used, mainly for ease of assembly are ordinary through hole thin film resistors (burn resistors).

For robustness and reliability, the thermal response of the mechanism must be well understood. This became apparent during the earliest development tests of the ADM. To reach the melting point of the dyneema the power dissipated in the burn resistors must generally exceed the maximum rating of the component for a short period. Therefore, choosing the operating current and operating time is a careful trade-off between ensuring that the resistor reliably cuts the meltline, and also ensuring that the resistor itself, the solder joints, PCB and any other components nearby are not damaged by the high temperatures involved.

These choices are further complicated by the requirement that the mechanism operates over a wide range of environmental temperatures. The burn resistor must get hot enough to cut the meltlines at the lowest expected operating temperature but not hot enough to cause damage at the highest expected operating temperature. When testing at ambient, heat lost from the resistors by convection may also considerably change the thermal response from that seen in vacuum.

A thermal vacuum test campaign was carried out to better understand and characterise the thermal behaviour of the ADM. The main objectives for this test were

1. to compare the performances of the mechanism in ambient and in vacuum conditions at different operating temperatures,
2. to investigate the effect of the meltlines on the temperature reached by the burn resistors, and
3. to stress test the mechanism by carrying out several burn tests over several thermal cycles.

For the test a special model of the ADM was built with additional PT1000 temperature sensors installed on the module. Two of these sensors were installed directly on the body of the burn resistors using a thermally conductive epoxy. This test was carried out in conjunction with an acceptance test for another satellite subsystem, which dictated the temperature limits. During the test, burns of the resistors were performed in vacuum at temperatures between -37C and +56C. The test shows many interesting results including the effect of the dyneema lines on the thermal response, the possibility of desoldering the burn resistors, and a comparison between ambient and vacuum conditions.

This paper is structured as follows. Section 2 gives a more detailed description of the device

under test, its operation and the installed temperature sensors. Section 3 describes the temperature profile used for the TVAC test and when different tests of the mechanism were carried out. Section 4 presents and discusses the main results of the tests. In Section 5 the main conclusions of the work are summarised including a list of the key technical challenges associated with this type of mechanism and recommendations that will help make future designs more robust and reliable.

2. Test Item Description

The ADM has an aluminium base which supports the mechanical components. The main X-shaped PCB which contains the module electronics is mounted in this base. Figure 1 shows a single HDRM. This is replicated four times, at each corner of the module, one for each antenna element. The four antenna elements are attached to spring actuated doors which are held closed by the meltlines. Each mechanism has two meltlines and two burn resistors (primary and secondary) for redundancy, in case one line should break prematurely or one resistor should not operate correctly. Good contact between the lines and the bodies of the resistors is ensured by the tensioning springs and by passing each line over the primary resistor and under the secondary resistor as shown. The dumbbell shape of the burn resistor also helps to centre the meltlines on the body. Each coiled element also presses a switch that detects when it is successfully deployed.

The burn resistors have a nominal value of 82 ohms and are operated at 12V, dissipating a nominal 1.76W. Primary and secondary resistors are operated by independent control chains to maximise redundancy. The module has two 12V inputs. The primary resistors use one of these 12V inputs but are switched on independently by transistors on the module. The secondary resistors are connected in parallel directly to the other 12V input and so must always operate together.

For the characterisation test, four PT1000 temperature sensors were installed on the module. Figure 2 shows two of these viewed from the top of the module. Sensor 1 is attached directly to the top side of X+ secondary burn resistor. Sensor 2 is attached to the underside of the Y+ primary burn resistor. The other two sensors are attached to the underside of the module. Sensor 3 is directly below the X- burn resistors and sensor 4 is attached to the centre of the PCB.

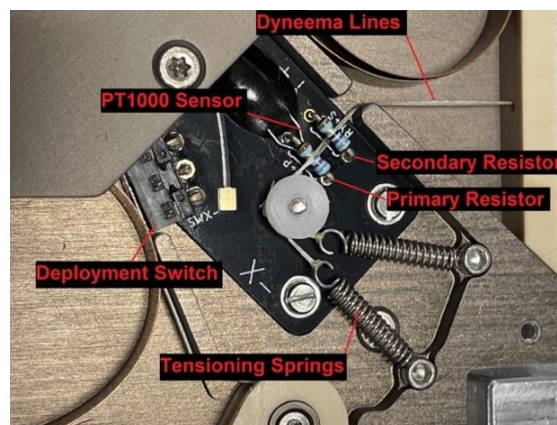


Figure 1. Overview of one HDRM present on the ADM.

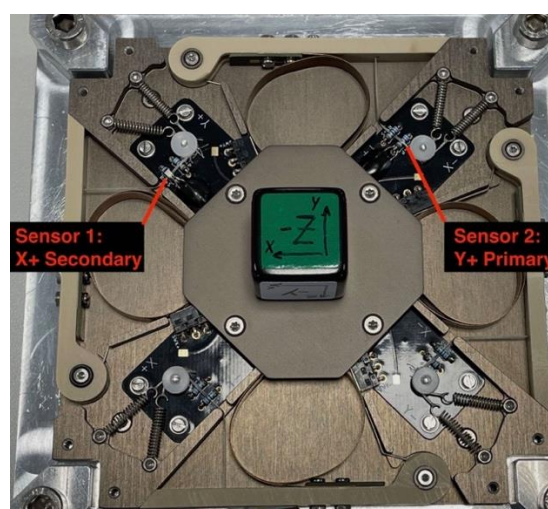


Figure 2. Top view of the ADM before TVAC test showing resistor sensor locations.

3. Test Setup and Test Profile

Before installation of the ADM in the chamber, deployment tests were carried out at ambient, first using the primary burn resistors and, after installation of new meltlines, using the secondary burn resistors. After a final reinstallation of the meltlines the module was installed in the vacuum chamber. During the entire test campaign, based on previous observations at ambient, a duration of 30 seconds was used for all burn tests.

Figure 3 shows the test setup inside the chamber. The primary method of heat transfer to the test item is conduction through a thermal plate mounted in the centre of the chamber. A thermal shroud also surrounds the test item for heat transfer via radiation. For the test, the module was mounted on an aluminum adapter plate. This adapter plate was then bolted to the thermal plate. Copper spacers were used between the adapter and the thermal plate to ensure good conduction while allowing space for the harnesses which were routed from the

bottom of the module to pass-throughs on the side of the chamber.

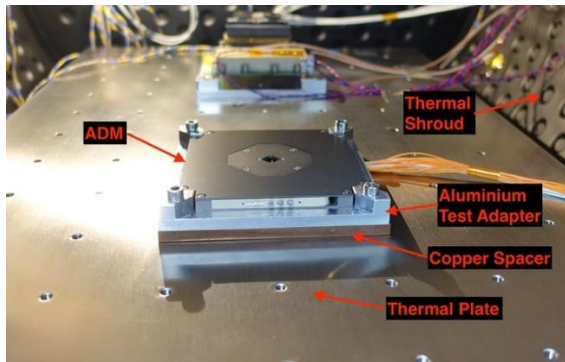


Figure 3. ADM mounted inside the chamber.

On the outside of the chamber the ADM was connected to custom built EGSE which allowed operation of the module and logging of voltages, currents and PT1000 temperatures.

After pump down of the chamber, the temperature profile followed for the test was dictated by the acceptance test of the EIRSAT-1 radio transceiver which took place at the same time. Figure 4 shows the thermal plate temperature and chamber pressure as measured throughout the test. The test consisted of four full cycles from cold to hot and then back to ambient temperature. Also shown in Figure 4 are the times at which burn tests were carried out in the chamber.

As refurbishment of the ADM is not possible without repressurising the chamber, it was only feasible to perform one burn test with meltlines installed for each antenna element. It was decided to carry out these tests at the coldest part of the profile, after the first cold dwell period at -40C (burns 1-4 in Fig. 4). After these tests, several more burn tests were completed at

different parts of the cycle to assess the response without meltlines and further stress the module. The most burn tests were carried out for the resistors with temperature sensors installed, i.e. the Y+ primary resistor and the X+ secondary resistor (with all secondary resistors operating together). In total 134 burns were carried out, 54 with secondary resistors and 80 with the primary resistors, 57 for Y+, 8 for Y-, 8 for X+, and 7 for X-.

4. Results

4.1. Deployment tests at ambient and after the first cold dwell in vacuum

Table 1 lists the results of deployment tests carried out at ambient before placing the ADM in the chamber and at the end of the first cold dwell in vacuum. During the ambient deployment tests all elements deployed successfully for both primary and secondary resistors. For the primary burn tests, the deployment times for the X- and Y+ elements are longer than the 3-4 seconds that have typically been seen during ambient testing of the module. This is not surprising however and is most likely due to the addition of the temperature sensors on the Y+ resistor and on the PCB directly underneath the X- resistor. The sensors and thermally conductive epoxy reduce the thermal isolation between the resistor bodies and the PCB meaning they are not as effective at cutting the line. Ideally, a non-contact temperature measurement would be used to measure the resistor temperature. However, this is not feasible in the vacuum chamber. For the secondary burn tests at ambient, again the X+ showed a longer than typical deployment time. Again, this is likely due to the addition of the temperature sensor directly on the resistor body.

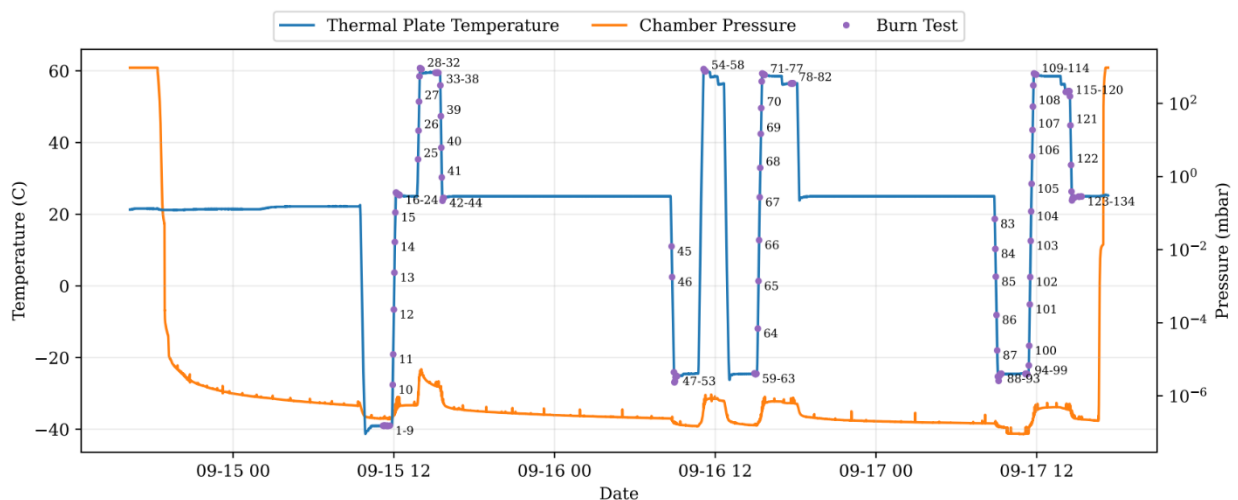


Figure 4. TVAC temperature and pressure profile showing times that burn test were carried out.

In vacuum the first two deployment tests were carried out using the Y+ and Y- primary resistors. Again, the resistor with the sensor installed (Y+) took longer to deploy at 22.8 seconds. The Y- element deployed after 9.9 seconds. The next burn test used the secondary resistors, with X- and X+ elements still stowed. During this test the X- element deployed at 20.1 seconds but the X+ remained stowed after the 30s burn had completed. Again, this is probably due to the reduced performance caused by adding the sensor. Finally, the X+ primary resistor was used to deploy the remaining element, taking 10.3 seconds.

Table 1. Deployment test results at ambient and after first vacuum cold dwell.

Burn Resistor	Average Current (A)	Switch Times (s)			
		Y+	Y-	X+	X-
Ambient					
Y+ Pri.	0.144	6.6	-	-	-
Y- Pri.	0.143	-	4.2	-	-
X+ Pri.	0.144	-	-	4.3	-
X- Pri.	0.144	-	-	-	5.3
Sec.	0.584	3.0	3.7	6.5	3.7
Vacuum First Cold Dwell					
Y+ Pri.	0.145	22.8	-	-	-
Y- Pri.	0.145	-	9.9	-	-
Sec.	0.581	-	-	-	20.1
X+ Pri.	0.145	-	-	10.3	-

4.2. Resistor temperature profiles in ambient and vacuum, with and without meltlines

Figure 5 shows the temperature of the Y+ primary resistor during burns at ambient and after the first cold dwell, both with and without meltlines in place. Here the effect of the dyneema lines on the temperature reached by the burn resistors is clear, seen as the difference between the dashed and solid lines. For the vacuum burn the breaking of the first meltline can be clearly seen, with a change in conduction of heat away from the resistor. Then, approximately 2.5 seconds later the breaking of the second line can be seen, coinciding with the deployment switch activation and again with a change in heat transfer characteristics from the resistor.

Figure 5 also shows a significant difference in performance in vacuum vs. ambient conditions. The rise in temperature of the body of the burn resistors after 30 seconds in vacuum (229C) is 50C greater than that achieved in ambient conditions (179C).

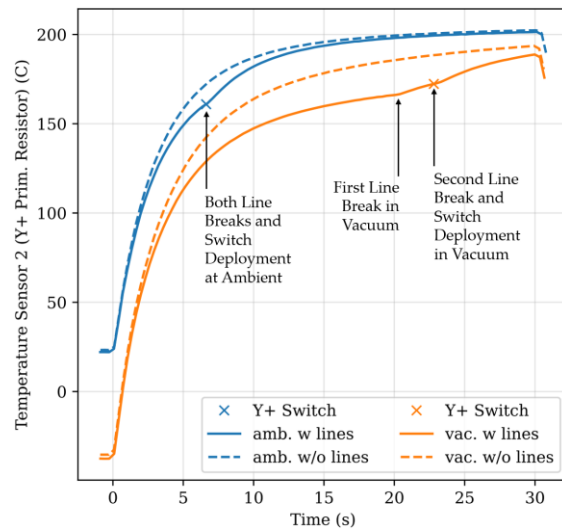


Figure 5. Resistor temperatures during burns in ambient and after vacuum cold dwell.

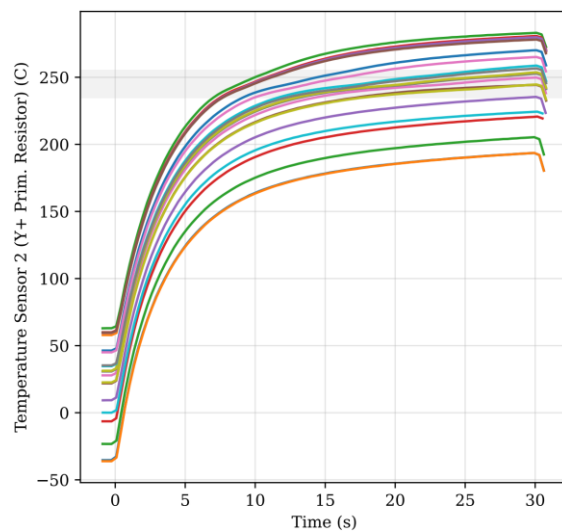


Figure 6. Y+ resistor temperatures during burns over a range of starting temperatures. The region where desoldering occurs is highlighted.

4.3. Performance at high temperatures

After removing the ADM from the chamber, the cover of the module was removed to inspect inside. It was noted that there was a small ball of solder that had adhered to the outer cover. In addition, it was noted that one of the resistors in this area had dropped to a lower height above the PCB surface. This would suggest that during burns at high temperature the resistors legs may get hot enough to reflow the solder joints connecting them to the PCB. The solder used has a melting point of approximately 183C. Figure 6 shows the temperature curves for the first 20 burn tests carried out using the Y+ primary resistor. Here we can clearly see a flattening of the curves when the temperature reaches approximately 250C. This suggests that when the body of the resistor reaches this

temperature the legs are then hot enough to reflow the solder joints and the latent heat required for melting causes the observed flattening of the heating curve.

5. Discussion and Conclusions

During the TVAC test it was shown that this HDRM can operate successfully in vacuum at temperatures between -37C and +56C. The burn resistors were shown to be very robust to repeated operation over this range of temperatures without failure, with a total of 134 burn tests being carried out.

A major technical challenge for this type of HDRM, particularly if using off-the-shelf components is to design it to operate successfully over the full range of possible operating temperatures on orbit. At low temperatures the change in temperature of the resistor during a burn must be maximised so that it breaks the meltlines. To help with this the width of the PCB traces supplying current to the resistors should be as small as possible to maximize the thermal isolation of the resistor bodies while also being able carry the required current. At high temperatures the resistors must not get so hot that they breakdown, reflow the solder joints or damage the PCB or nearby components. In this test it was shown that the components themselves are very robust, but solder reflow is an issue. To avoid this a solder alloy with higher melting point should be used for the resistor joints. One such alloy, approved by ECSS is 10% tin 90% lead. Alternatively, the burn time could be adjusted, or power modulated depending on the ambient temperature, or the resistors could be switched off when notified by the switch of a successful deployment. However, all these solutions add complexity and possible points of failure for what is generally a mission critical mechanism.

During the test It was observed that the delta T achieved by the burn resistors in vacuum is 50C greater than that at ambient, due to the absence of convection. This must be considered early in the design stage as components that work well in ambient will likely face higher extremes of temperature in vacuum.

Finally, the effect of the meltlines in conducting heat away from the burn resistors cannot be neglected, as clearly seen in Fig. 5. Therefore, it is advantageous to use a line with the smallest diameter possible. In the testing phase, the correct number of meltlines should always be installed. A mechanism that operates successfully with a single line may not deploy when a second is installed.

Acknowledgements

The authors acknowledge all students who have contributed to the EIRSAT-1 project. EIRSAT-1 is supported by ESA's Education Office under the FYS! 2 programme. MD, DM, JT, RD and LS acknowledge support from the Irish Research Council under grants GOIPG/2018/2564, GOIPG/2014/453, GOIPG/2014/684, GOIPG/2019/2033 and GOIPG/2017/1525, respectively. GF acknowledges support from a scholarship associated with the UCD Ad Astra fellowship programme. DM, AU, JM and SMcB acknowledge support from Science Foundation Ireland (SFI) under grant 17/CDA/4723. SW acknowledges support from ESA under PRODEX contract number 400012071. JE and JR acknowledge scholarships from the UCD School of Physics. FM acknowledges support from the UCD School of Computer Science. LH acknowledges support from SFI under grant 19/FFP/6777 and support from EU H2020 AHEAD2020 project (grant agreement 871158). This study was supported by ESA's Science Programme under contract 4000104771/ 11/NL/CBi and by ESA's PRODEX Programme under contract number C 4000124425.

References

- [1] G. F. Brouwer, W. J. Ubbels, A. A. Vaartjes, and F. T. Hennepe, "Assembly, integration and testing of the DELFI-C3 nanosatellite," in *59th IAC*, no. IAC-08-D1.5.6, Glasgow, Scotland, Oct. 2008.
- [2] S. Jeon and T. W. Murphey, "Design and analysis of a meter-class cubesat boom with a motor-less deployment by bi-stable tape springs," in *52nd AIAA/ASME/ASCE/AHS/ASC Structures, Structural Dynamics and Materials Conference*, Denver, CO, 2011, pp. 1–11.
- [3] S. Damkjar, C. Cupido, C. Nokes, I. R. Mann and D. G. Elliott, "Design and Verification of a Robust Release Mechanism for CubeSat Deployables," 2019 IEEE Canadian Conference of Electrical and Computer Engineering (CCECE), 2019, pp. 1-4, doi: 10.1109/CCECE.2019.8861795.
- [4] S. Walsh et al. "Development of the EIRSAT-1 CubeSat through Functional Verification of the Engineering Qualification Model," *Aerospace*, 8(9), 254, 2021
- [5] J. Thompson et al. "Double dipole antenna deployment system for EIRSAT-1, 2U CubeSat," In *Proceedings of the 2nd Symposium on Space Educational Activities*, Budapest, Hungary, 11–13 April 2018; pp. 221–225.